

Substrate-led cholesterol extraction from supported lipid membranes

Supplementary information

1) Characterization of the PDMS substrate

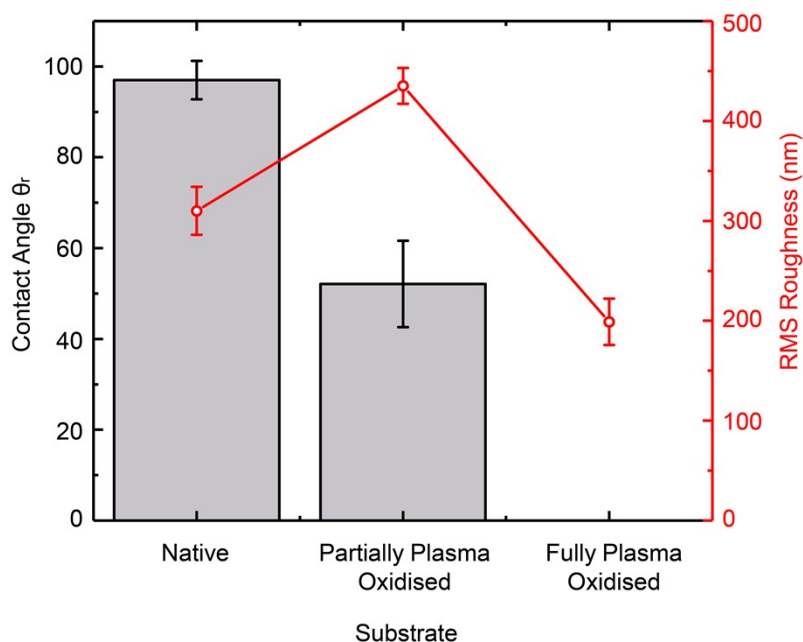


Figure S1 Change in surface chemistry and topography of PDMS during plasma oxidation. Comparison of change in root mean square roughness (red) and contact angle (grey) between fully plasma-oxidised, partially plasma-oxidised and native PDMS samples. The surface roughness was averaged from several 1 μm AFM scans of the PDMS surface, taken from different areas across the sample surface. All measurements were done in aqueous environment, under the same experiment condition used in cholesterol depletion measurements.

2) Statistical procedure for the analysis of the cholesterol extraction events

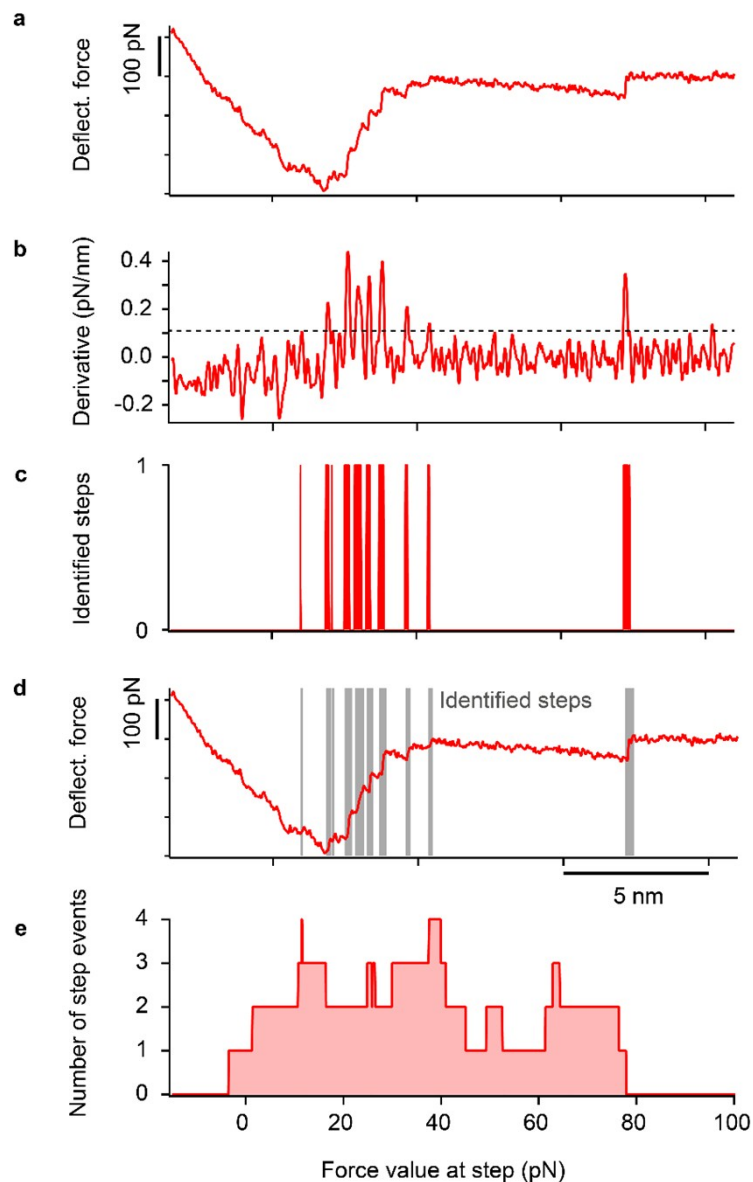


Figure.S2 Illustration of the semi-automated procedure used to analyse the AFM spectroscopy extraction curves. To objectively analyse a curve exhibiting steps **(a)**, a smoothing derivation is first applied by sliding a rod along the whole curve and plotting its slope **(b)**. Practically, the length of the rod is taken to be insensitive to the force fluctuations of the curve's baseline (here 8 points long) and a linear fit of the curve is done of a sliding interval corresponding to the rod's length. A thresholding procedure is then applied to the derivative whereby only parts of the curve above a threshold of two standard deviations of its average value are retained **(c)**. The results of the step identification process can be visualised in **(d)**. While the above parameters were used for the vast majority of curves, the outcome of each analysis was controlled visually, and the parameters finely adjusted if necessary. With each step (11 in the present case) the associated force change is calculated by comparing the force at both extremes of the step interval. Taking relatively large intervals as visible in **(c-d)** allows minimisation of potentially erroneous force measurements at the step itself due to force spikes or

instabilities. The results are then compiled into a histogram **(e)** where the bin width represents two standard deviation of the force detection baseline in the absence of any step (15 pN). The histogram may hence give a non-zero probability to negative forces if the step reported is within 15 pN of zero. The histograms for each curve analysed are subsequently combined in a complete histogram, as presented in Figure 2 f, i, l.

3) Model fit used to quantify the extraction of cholesterol from DOPC:Chol bilayers

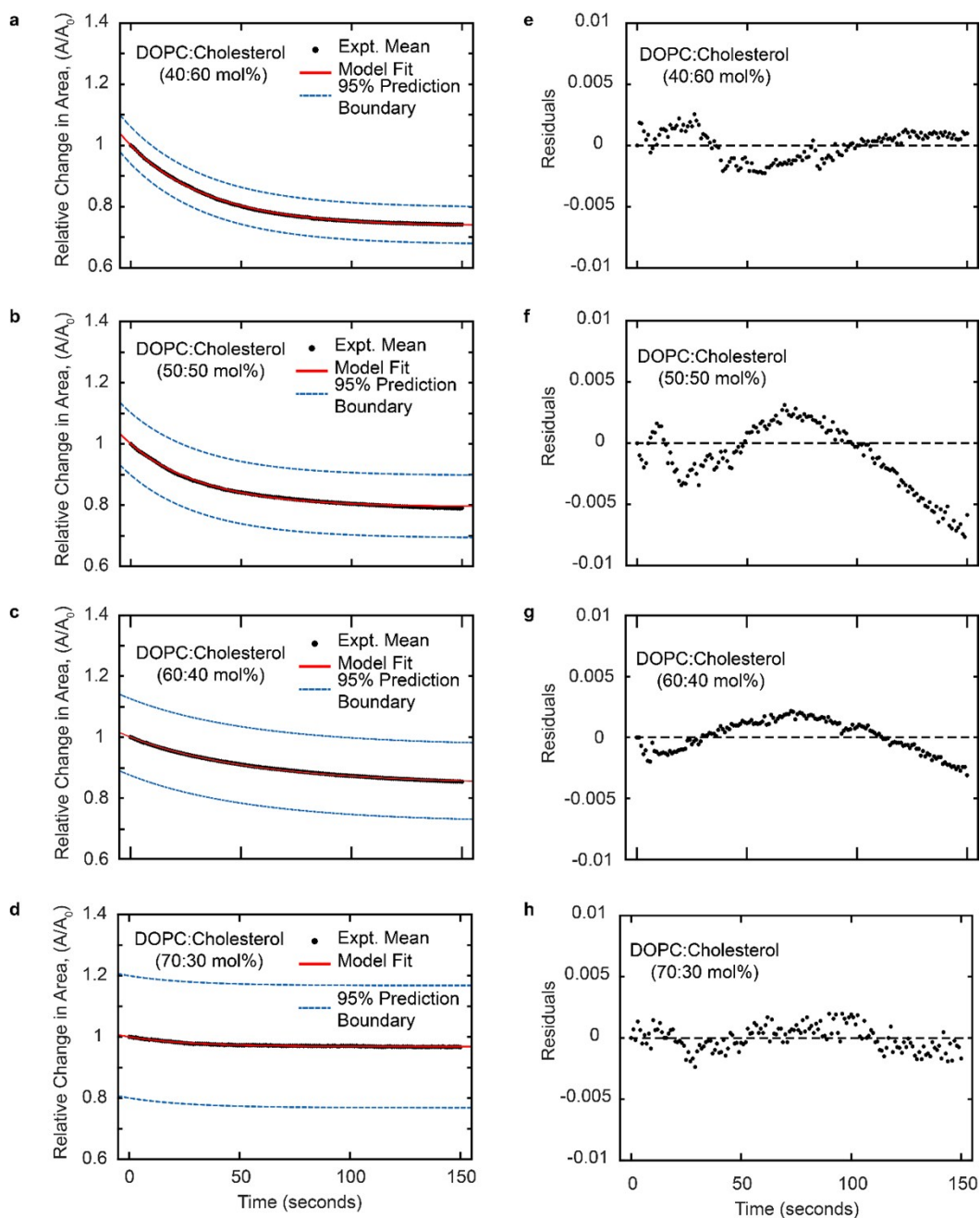


Fig. S3 Quality of fits of the experimental data in Fig. 3 to the cholesterol depletion model presented in the main text. Experimentally measured (black) and theoretically predicted (red) areas of DOPC patches with (a) 0.6, (b) 0.5 (b), 0.4 (b) and 0.3 (d) cholesterol mole fractions, supported on partially oxidised PDMS. Experimental data averaged from $n=20,15,15,16$ different patches for cholesterol mole fractions 0.6, 0.5, 0.4 and 0.3 respectively. Blue lines indicate the 95% confidence bounds. Residuals for each model fitting for 0.6 (e), 0.5 (f), 0.4 (g) and 0.3 (h) cholesterol mole fraction data sets.

Table S1. Extracted values for accessible cholesterol mole fraction and cholesterol depletion rate constant.

Mole Fraction, χ_{Chol}	Accessible cholesterol mole fraction, χ_{acc}	Depletion rate constant, k (s-1)
0.3	0.099 ± 0.005	0.0360 ± 0.0006
0.4	0.350 ± 0.012	0.0191 ± 0.0001
0.5	0.387 ± 0.007	0.0314 ± 0.0002
0.6	0.429 ± 0.004	0.0292 ± 0.0001

The experimental means of each cholesterol mole fraction data sets (Fig. 1) were fitted to the model presented in Equation 1 in the main text. The weights used to fit the model were derived from the standard deviation. The fits of the experimental data to the model allow us to extract values for the accessible cholesterol mole fraction, $\chi_{acc}^{(0)}$, at t=0 and the depletion rate constant k in DOPC:Chol lipid patches with 0.3, 0.4, 0.5 and 0.6 initial cholesterol mole fractions.

4) Changes in the lipid patches and the PDMS substrates during mechanical strain cycles

During the stretching cycle the DOPC:Chol patches lose on average 2-5% more area than when supported on partly oxidised PDMS (Fig. 4). Control experiments show that pure DOPC bilayers also lose on average 5% of their surface area during a strain cycle of similar amplitude (Fig. S4a). This indicates that the stretching may not only affect the cholesterol population in the bilayer. Interestingly upon subsequent strain cycles the area of the same DOPC patches remain largely unaffected (Fig. S4b). This suggests that the patches may be arrested in a high-energy state after the violent process of vesicle fusion and their initial area might be slightly larger than their equilibrium area. The application of mechanical strain cycle allows the vesicles to find lower energy state and thus the patches slightly shrink during the first strain cycle.

However, depletion of other membrane components may not be fully excluded. This could be facilitated by the larger cracks that open in the PDMS substrate following mechanical stretch (Fig. S5a-c). These cracks may be able to extract also DOPC molecules and the much larger Rhodamine-DPPC fluorophores. Such non-specific lipid extraction is likely to play a role at very large strain magnitudes (> 35%) where we occasionally observe the formation of micron scale PDMS surface fissures, which fill up with fluorescent membrane from the contacted patch and fully disrupt it (Fig. S5d-f).

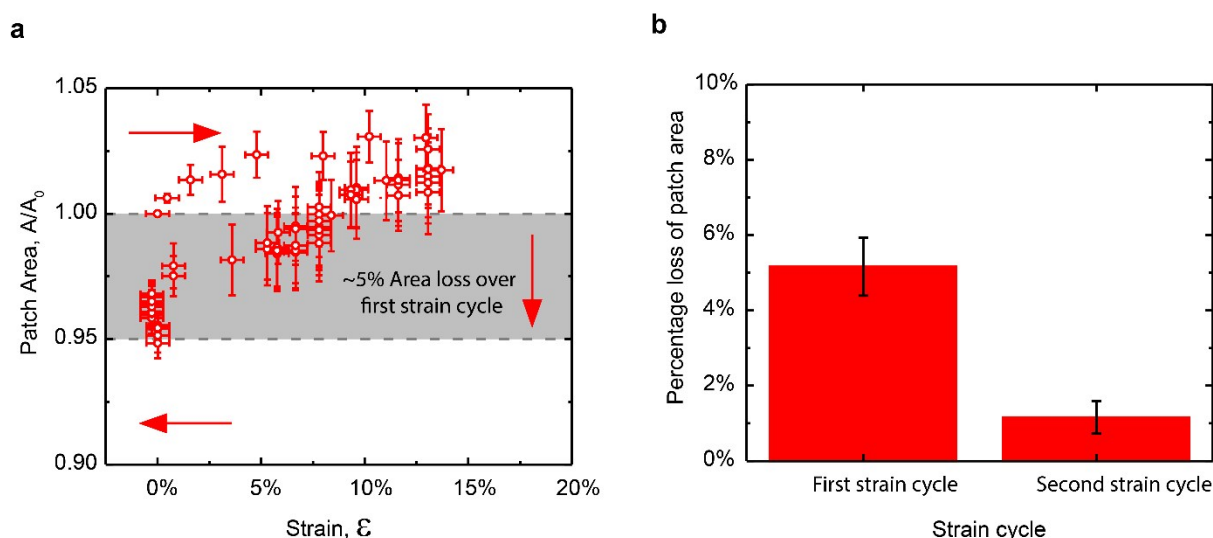


Fig. S4 Area changes in DOPC lipid bilayer area during expansion/compression cycles. (a) Area changes in $n=9$ independent DOPC lipid patches as a function of substrate strain, ϵ . The arrows indicate the direction of the strain cycle. **(b)** A bar chart of percentage area loss for $n=10$ independent DOPC lipid patches after the first and second applications of substrate strain cycles. We report an area change of $-5.2 \pm 0.8\%$ after the first strain cycle and -1.2 ± 0.4 for the second cycle.

5) Evidence of nanoscale and microscale surface cracking on PDMS substrates

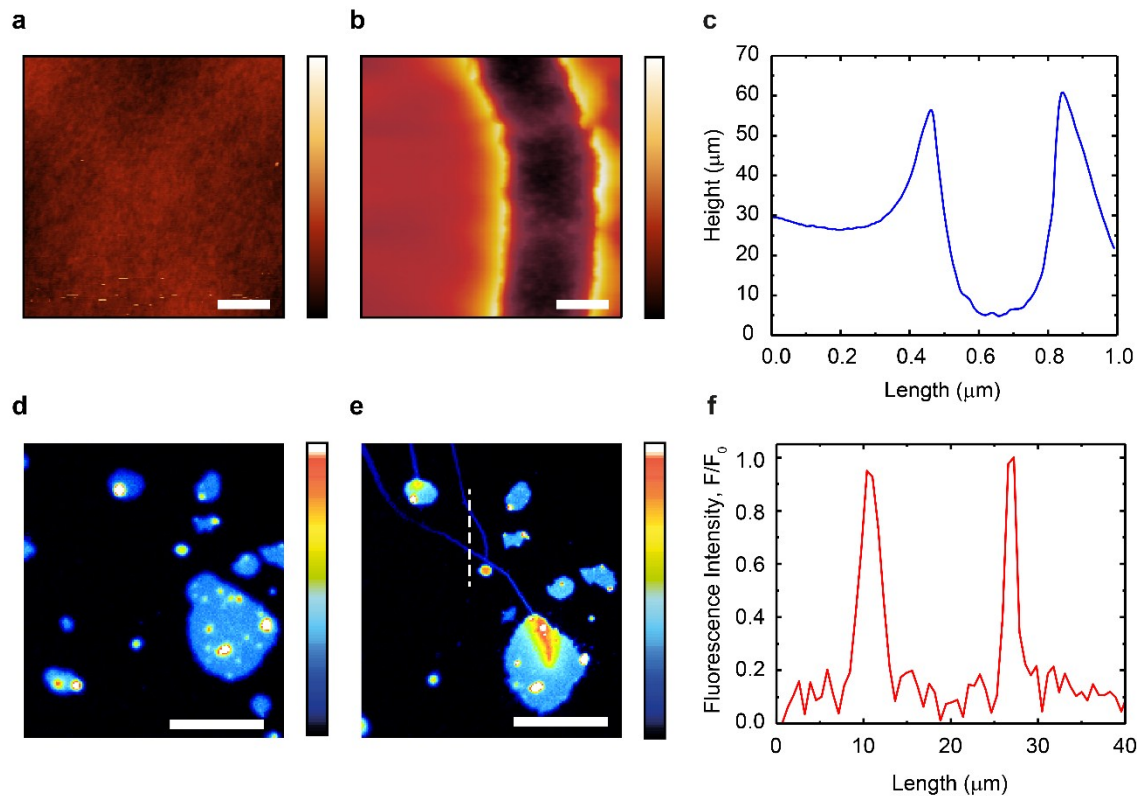


Fig. S5 Evidence of nanoscale and microscale surface cracking on PDMS substrates. AFM scans of fully plasma-oxidised PDMS substrate **(a)** before and **(b)** after the application of 15% tensile. **(c)** A line profile of the crack shows a crack diameter of ~ 300 nm. **(d-e)** Fluorescent images of DOPC:Chol lipid patches (40:60 mol% doped with 0.1 mol% Rh-DPPE) on PDMS stretching device. Images show substrate **(d)** before and **(e)** after a 35% tensile is applied, and micron scale surface cracking is evident. The cracks become fluorescent as Rh-DPPE is able to invade the fissure. **(f)** A line profile taken from image **(e)** shows cracks with a diameter of ~ 5 μm . Scalebar 200 nm in **(a,b)** and 20 μm in **(d-g)**. Colour scale on **(d-g)** fluorescence in arbitrary units.